ELSEVIER

Inorganica Chimica Acta 264 (1997) 269–278

Inorganica Chimica Acta

Electronic and molecular structure of 2,2′-bipyrimidine-bridged bis(organoplatinum) complexes in various oxidation states. Radical-bridged diplatinum species and the absence of a Pt(III)/Pt(II) mixed-valent intermediate

Axel Klein [a], Wolfgang Kaim [a,*], Fridmann M. Hornung [a], Jan Fiedler [b], Stanislav Zalis [b]

[a] *Institut für Anorganische Chemie, Universität Stuttgart, Pfaffenwaldring 55, D-70550 Stuttgart, Germany*

[b] *J. Heyrovsky Institute of Physical Chemistry, Academy of Sciences of the Czech Republic, Dolejškova 3, CZ-18 000 Prague 8, Czech Republic*

Received 4 March 1997; revised 2 April 1997; accepted 2 June 1997

Abstract

Dinuclear organoplatinum compounds $R_nPt(bpym)PtR_n$ ($R = Me =$ methyl, $n = 2, 4$; $R = Mes =$ mesityl, $n = 2$; bpym = 2,2′-bipyrimidine) were prepared and characterized. The neutral compounds and their neighboring oxidation states were studied using cyclic voltammetry, ^1H NMR or EPR spectroscopy and UV–Vis spectroelectrochemistry. Oxidation state assignments based on these data could be made for the following compounds: $R_2Pt^{II}(bpym)Pt^{II}R_2$, $[R_2Pt^{II}(bpym^{-I})Pt^{II}R_2]^{\bullet -}$, $[R_2Pt^{II}(bpym^{-II})Pt^{II}R_2]^{2-}$, $[Mes_2Pt^{III}(bpym)Pt^{III}Mes_2]^{2+}$, $Me_4Pt^{IV}(bpym)Pt^{IV}Me_4$, $[Me_4Pt^{IV}(bpym^{-I})Pt^{IV}Me_4]^{\bullet -}$. The two-electron oxidation of $Mes_2Pt(bpym)PtMes_2$, i.e. the absence of a stable Pt(III)/Pt(II) mixed-valent state, confirms that the highest-lying occupied metal orbitals (d_{z^2}) do not communicate via the π system of the bridging ligand. A crystal structure analysis of photoreactive $Me_4Pt^{IV}(bpym)Pt^{IV}Me_4$ was obtained: space group *Pbca*, $a = 12.830(2)$ Å, $b = 11.502(2)$ Å, $c = 12.877(2)$ Å, $V = 1900.3(5)$ Å^3, $Z = 4$. The structural refinement revealed elongated axial Pt–methyl bonds of about 2.13 Å. The structural features could be well reproduced by a DFT calculation of $H_4Pt^{IV}(bpym)Pt^{IV}H_4$ which also confirmed the σ character of the HOMO. Of the ligand-reduced systems, the Pt(II) species exhibits a higher degree of g anisotropy than the Pt(IV) species. Low-lying excited states of the species generated were assigned through information from vibrational structuring, solvatochromic behavior and from (spectro)electrochemical results. © 1997 Elsevier Science S.A.

Keywords: Crystal structure; Dinuclear complexes; Platinum complexes; Alkyl complexes; Bipyrimidine complexes; Spectroelectrochemistry; Organometallics

1. Introduction

Pt(II) and Pt(IV) complexes with nitrogen donor-containing ligands have found interest as chemotherapeutic agents (cytostatica) [1], catalysts [2], and photoemissive [3] and redox-active [4] species. The latter often involve π-accepting chelate ligands of the α-diimine type such as aromatic 2,2′-bipyridine [3i,4c,f] or non-aromatic 1,4-diaza-1,3-butadienes [4e]. Detailed photophysical studies [3], calculations [3d], structure determinations [3c,d,4c,e] and (spectro)electrochemical and EPR studies of the generated paramagnetic species [4] have been used recently to elucidate the nature of these systems (α-diimine)PtX_n in ground, reduced, oxidized and low-lying excited states. The latter may include ligand-field (LF) and metal-to-ligand charge transfer (MLCT) excited states [3], with particular emphasis on possible intermolecular interactions in square-planar systems (α-diimine)PtX_2 [3f,i,o]:

$$(\alpha\text{-diimine})Pt^kX_n + e^- \rightarrow [(\alpha\text{-diimine}^{-I})Pt^kX_n]^{\bullet -}$$

reduction

$$(\alpha\text{-diimine})Pt^kX_n - e^- \rightarrow [(\alpha\text{-diimine})Pt^{k+1}X_n]^{\bullet +}$$

oxidation

$$(\alpha\text{-diimine})Pt^kX_n + h\nu \rightarrow [(\alpha\text{-diimine}^{-I})Pt^{k+1}X_n]^*$$

MLCT excitation

Considering the electronic complexity of these compounds [3,4] the use of organic substituents as co-ligands X seems attractive due to the greater variability of such groups. For instance, the use of axially protecting mesityl (Mes, 2,4,6-

---

[*] Corresponding author. Tel.: +49 711 685 41070/71; fax: +49 711 685 4165.

0020-1693/97/$17.00 © 1997 Elsevier Science S.A. All rights reserved
PII S0020-1693(97)05704-6

trimethylphenyl) substituents in compounds (α-diimine)-$PtMes_2$ has allowed us to avoid the undesired addition of nucleophiles to the one-electron oxidized monomeric Pt(III) states $[(\alpha\text{-diimine})PtMes_2]^+$ [4c,f]. It was thus possible to obtain spectroelectrochemical data on monomeric organometallic Pt(III) systems [4f] and to use the corresponding Pt(II)/Pt(III) half-wave potentials in correlations between optical data (absorption, emission energies) and electrochemical results [4f].

Electrochemically interesting metal/ligand combinations offer additional facets if they are part of a dinuclear or oligonuclear arrangement [5,6]. Oligonuclear Pt complexes have thus been known to form unusual structures [7a] and oxidation states [7b–g], including Pt^{III}/Pt^{II} mixed-valent dimeric forms [8]. Dinuclear Pt compounds have also been found to exhibit special cytostatic properties [9].

We now wish to present results for dinuclear organoplatinum complexes which contain 2,2′-bipyrimidine (bpym) as a conjugated bridging ligand. The bpym system has been commonly used to promote metal–metal interactions in dimetallic or oligometallic coordination compounds [10]; it is fairly rigid and keeps the two metal sites oriented towards each other at a distance of about 5–6 Å [10]. The syntheses and physical properties of some bpym-bridged bis(organoplatinum) compounds have been reported before [4a,11,12]; in this work we present the following set of dinuclear Pt^{II} and Pt^{IV} starting materials and describe the electronic structures of reduced, oxidized and MLCT excited states:

$R_nPt(bpym)PtR_n$ ($R=Me$, $n=2, 4$; $R=Mes$, $n=2$)

The methyl group (Me) as the most simple organic substituent and the mesityl (Mes) function as an axially protecting aryl group were used as organic co-ligands. Particular attention will be given to the question of metal–metal interaction and to the suitability of calculations (ab initio or density functional theory, DFT) to reproduce experimental structures for model compounds.

2. Experimental

2.1. Syntheses

2.1.1. Materials and procedures

The Pt precursor complexes $(DMSO)_2PtMes_2$ [13], $Pt_2Me_8(\mu\text{-}SMe_2)_2$ [14] and $Pt_2Me_4(\mu\text{-}SMe_2)_2$ [15], and the complexes $(\mu\text{-bpym})[PtMe_n]_2$ ($n=2, 4$) [11], were obtained following literature procedures. All preparations and physical measurements were carried out in dried solvents under an argon atmosphere, using Schlenk techniques. Furthermore, the tetramethylplatinum(IV) compounds had to be prepared and studied in the absence of intense light.

2.1.2. $Mes_2Pt(\mu\text{-}bpym)PtMes_2$

An amount of 295 mg (0.5 mmol) of dimesitylbis(dimethylsulfoxido)platinum(II) was suspended together with 39.5 mg (0.25 mmol) of 2,2′-bipyrimidine in 70 ml toluene and heated under reflux for 5 days. The sulfoxide vibration $\nu(S{=}O)$ at 1130 cm^{-1} of the Pt precursor complex [16] had disappeared by then. At the end of the reaction the temperature was lowered within a further day to accomplish slow precipitation of the product. The brown solid was collected on a microporous frit and washed with diethyl ether. Thus, we obtained a dark-brown microcrystalline powder. Yield 230 mg (90%). *Anal.* Found: C, 51.18; H, 4.89; N, 5.45. Calc. for $C_{44}H_{50}N_4Pt_2$: C, 51.56; H, 4.92; N, 5.47%.

2.1.3. $Mes_2Pt(\mu\text{-}bpym)PtMe_4$

A solution containing 54.5 mg (0.092 mmol) of the mononuclear complex $(bpym)PtMes_2$ [4f] and 32 mg (0.05 mmol) of $Pt_2Me_8(\mu\text{-}SMe_2)_2$ in 10 ml acetone was stirred for 5 h at ambient temperature in the absence of light. After removal of the solvent the black residue was suspended in 10 ml of diethyl ether and filtered through a microporous glass frit. The residue on the frit was dissolved in acetone and the acetone solution was slowly concentrated by evaporation, yielding a black microcrystalline solid. Yield: 68 mg (87%). *Anal.* Found: C, 42.4; H, 4.69; N, 6.27. Calc. for $C_{30}H_{40}N_4Pt_2$: C, 42.55; H, 4.76; N, 6.62%.

2.1.4. $Mes_2Pt(\mu\text{-}bpym)PtMe_2$

A solution containing 54.5 mg (0.092 mmol) of the mononuclear complex $(bpym)PtMes_2$ [4f] and 28.7 mg (0.05 mmol) of $Pt_2Me_4(\mu\text{-}SMe_2)_2$ in 10 ml acetone was stirred for 5 h at ambient temperature in the absence of light, producing a dark-purple precipitate. Filtration and washing with diethyl ether yielded a dark microcrystalline powder which was rather insoluble in all common solvents. Yield: 71 mg (94%). *Anal.* Found: C, 40.84; H, 3.98; N, 6.81. Calc. for $C_{28}H_{34}N_4Pt_2$: C, 41.17; H, 4.20; N, 6.86%.

2.2. Instrumentation

EPR spectra were recorded in the X-band on a Bruker System ESP 300 equipped with a Bruker ER035 M gaussmeter and a HP 5350 B microwave counter. ^1H NMR spectra were taken on a Bruker AC 250 spectrometer. UV–Vis–NIR absorption spectra were recorded on Shimadzu UV160 and Bruins Instruments Omega 10 spectrophotometers. Cyclic voltammetry and differential pulse voltammetry were carried out in dry solvents containing 0.1 M Bu_4NPF_6; a three-electrode configuration (glassy carbon working electrode, Pt counter electrode, Ag/AgCl reference) was used with a PAR 273 potentiostat and function generator with PAR M270/250 software. The ferrocene/ferrocenium couple served as internal reference. Spectroelectrochemical measurements were performed using an optically transparent thin-layer electrode (OTTLE) cell [17] for UV–Vis spectra and a two-electrode capillary for EPR studies [18].

2.3. Calculations

The electronic structures of the complexes $R_nPt(\mu\text{-}bpym)PtR_n$ ($n=2, 4$; $R=H, CH_3$) were studied using the

Table 1
^{1}H NMR data of 2,2′-bipyrimidine and its organoplatinum complexes [a]

Compound	Chemical shifts					Solvent
	bpym-H			Co-ligands		
	4,4′	5,5′	6,6′	*m*-H	*o*-CH$_3$, *p*-CH$_3$	
bpym [b]	8.99	7.64	8.99			DMSO-d$_6$
(bpym)[PtMes$_2$]$_2$	8.51	7.95	8.51	6.51	2.39, 2.06	DMSO-d$_6$
(bpym)[PtMes$_2$]$_2$ [c]	8.82	7.59	8.82	6.68	2.43, 2.21	CD$_2$Cl$_2$
Mes$_2$Pt(bpym)PtMe$_4$ [d]	8.68	7.70	9.40	6.70	2.42, 2.22	CD$_2$Cl$_2$
				CH_3^{ax}	CH_3^{eq}	
				−0.48	1.08	CD$_2$Cl$_2$
(bpym)[PtMe$_4$]$_2$	9.25	7.82	9.25	−0.50	1.09	CD$_2$Cl$_2$

[a] No NMR spectra could be obtained for the compounds Me$_2$Pt(μ-bpym)PtMes$_2$ and (bpym)[PtMe$_2$]$_2$ due to poor solubility. Chemical shifts δ in ppm vs. TMS.

[b] Coupling constant $^3J = 4.8$ Hz.

[c] $^3J_{H4/H5} = {^3J_{H5/H6}} = 5.5$ Hz, $^4J_{Pt/m\text{-}H} = 15.6$ Hz, $^4J_{Pt/o\text{-}CH3} = 8.9$ Hz, $^4J_{Pt/H4,6} = 3.9$ Hz (^{195}Pt: 33.8% natural abundance, $I = 1/2$).

[d] The Pt(II) center is next to the 4,4′ positions of bpym: $^3J_{H4/H5} = 5.5$ Hz, $^3J_{H6/H5} = 5.4$ Hz, $^4J_{H6/H4} = 1.8$ Hz, $^4J_{Pt/m\text{-}H} = 16.0$ Hz, $^3J_{Pt/H6} = 10.8$ Hz, $^3J_{Pt/H4} = 4.9$ Hz, $^2J_{Pt/CH3ax} = 43.8$ Hz, $^2J_{Pt/CH3eq} = 75.8$ Hz.

Gaussian 94 program package [19] for ab initio and density-functional/Hartree–Fock (DFT/HF) hybrid calculations. Quasi-relativistic effective core pseudo-potentials and a correspondingly optimized set of basis functions [20] were used for the Pt centers. Within single-point calculations on Me$_4$Pt(μ-bpym)PtMe$_4$ and Me$_2$Pt(μ-bpym)PtMe$_2$ complexes Dunning's [21] valence double-zeta values with polarization functions were used for H, C and N atoms. The same basis sets were used for the geometry optimization of Me$_2$Pt(μ-bpym)PtMe$_2$ and of the H$_4$Pt(μ-bpym)PtH$_4$ model system. Due to the large size, the geometry of Me$_4$Pt(μ-bpym)PtMe$_4$ could be calculated only without polarization functions; however, the mononuclear analog (bpym)PtMe$_4$ could be calculated as described above. All calculations were performed in D_{2h} constrained symmetry where the μ-bpym ligand defines the *xy* plane and the Pt atoms lie on the *x* axis. Single-point calculations of Me$_4$Pt(μ-bpym)PtMe$_4$ were done with the experimental structure and those of Me$_2$Pt(μ-bpym)PtMe$_2$ within the optimized geometry. Within DFT/HF calculations the 'Becke-3-LYP' (B3LYP) potential has been employed [22].

2.4. Crystal structure analysis

Compound Me$_4$Pt(μ-bpym)PtMe$_4$ (C$_{16}$H$_{30}$N$_4$Pt$_2$; $M_r = 668.62$): Brown crystals were obtained by slow evaporation of a solution in tetrahydrofuran (THF)/toluene (1:1) in the dark at room temperature. Orthorhombic, *Pbca*, $a = 12.830(2)$, $b = 11.502(2)$, $c = 12.877(2)$ Å, $V = 1900.3(5)$ Å^3, $Z = 4$, $\rho_{ber} = 2.337$ g cm^{-3}, $T = 183(2)$ K, μ(Mo Kα) = 14.709 mm^{-1}, $F(000) = 1240$, Siemens P4 diffractometer with Mo Kα radiation ($\lambda = 0.710\,73$ Å). 5425 reflections with $5.72 \leq 2\Theta \leq 60°$ ($-18 \leq h \leq 18$, $0 \leq k \leq 16$, $0 \leq l \leq 18$), 2778 independent reflections. With 2680 observed reflections and no restraints a total of 100 parameters was refined: $wR = 0.1326$ [1], $R = 0.0510$ [2] ($I > 2\sigma(I)$), GOF = 1.057 [3]. The structure was solved by the Patterson method using the SHELXTL-Plus package [23a] and refinement was carried out with SHELXL-93 employing full-matrix least-squares methods on F^2 [23b]. A numerical absorption correction was applied using the DIFABS method [23c]; attempts at empirical absorption correction failed. All non-hydrogen atoms were treated anisotropically; hydrogen atoms were included using the riding model.

3. Results and discussion

3.1. Synthesis and general properties

The dinuclear organoplatinum compounds Mes$_2$Pt(bpym)PtMes$_2$, Mes$_2$Pt(bpym)PtMe$_2$, Mes$_2$Pt(bpym)PtMe$_4$, Me$_2$Pt(bpym)PtMe$_2$ and Me$_4$Pt(bpym)PtMe$_4$ were obtained according to established methods. Their identity was checked using elemental analysis and, unless insolubility precluded measurements [11,12], ^{1}H NMR spectroscopy (Table 1), the assignments being supported by coupling patterns involving the ^{195}Pt isotope (33.8% natural abundance, $I = 1/2$).

The very poor solubility of those complexes containing the PtMe$_2$ group probably has its origins in intermolecular interactions (stacking) of unencumbered square-planar Pt(II), especially in the bifunctional systems described here. Mesityl

---

[1] $wR = \{\Sigma[w(|F_o|^2 - |F_c|^2)^2]/\Sigma[w(F_o^4)]\}^{1/2}$.

[2] $R = (\Sigma\|F_o| - |F_c\|)/\Sigma|F_o|$.

[3] $\mathrm{GOF} = \{\Sigma w(|F_o|^2 - |F_c|^2)^2/(n-m)\}^{1/2}$; n = no. of reflections; m = no. of parameters.

substitution does not allow such a stacking [4c,f] and thus leads to much better soluble organoplatinum(II) compounds.

The pronounced photosensitivity of the tetramethylplatinum(IV) is attributed to the photolability of axial platinum–carbon bonds. We have pointed out previously [24] that metal–carbon σ bond combinations in conjugation with low-lying π* orbitals are prone to σ–π* charge transfer processes which result in homolysis of the then singly occupied organometal σ bond. EPR [25a] and photoreactivity studies [25b] involving the more simple 1,4-diaza-1,3-butadiene ligand system have been carried out.

3.2. *Calculation and crystal structure of $Me_4Pt(bpym)PtMe_4$*

An obvious indication concerning the photoreactivity mechanism is provided by the molecular structure of $Me_4Pt(bpym)PtMe_4$. The crystals, obtained by slow evaporation from THF/toluene solution, were subjected to X-ray diffraction and the structure was solved with the results given in Tables 2 and 3 (see also Section 2).

There are no significant intermolecular interactions between the centrosymmetric molecules of $Me_4Pt(bpym)PtMe_4$ in the crystal. The molecular structure (Fig. 1) confirms the bis-chelate coordination of the bpym bridging ligand [10] and reveals close to octahedral configuration with C–Pt–C angles between 87.1 and 90.9° at the metal centers [4e]. The small 'bite' angle N–Pt–N of 77.2° is related to the α-diimine chelate arrangement and the rather long Pt–N distances of about 2.15 Å; the metal–metal distance of 5.751 Å is typical for bpym-bridged dinuclear complexes [10].

Table 2
Atomic coordinates (×10⁴) and equivalent isotropic displacement parameters ($Å^2 \times 10^3$) for $Me_4Pt(bpym)PtMe_4$. U_{eq} is defined as one third of the trace of the orthogonalized U_{ij} tensor

	x	y	z	U_{eq}
Pt(1)	383(1)	2657(1)	678(1)	17(1)
C(1)	−437(7)	5060(9)	381(7)	19(2)
N(1)	−622(6)	4116(8)	974(6)	20(2)
C(8)	−276(8)	1517(8)	1682(8)	26(2)
C(4)	−1408(8)	4237(9)	1668(8)	23(2)
C(7)	1406(9)	1356(10)	293(10)	34(2)
C(3)	−2006(8)	5221(10)	1691(9)	30(2)
C(6)	1453(8)	3213(11)	1836(8)	31(2)
C(5)	−653(9)	2085(12)	−519(8)	32(2)
N(2)	−967(5)	6046(7)	370(6)	18(2)
C(2)	−1778(7)	6131(10)	1051(8)	23(2)

Table 3
Selected distances (Å) and bond angles (°) of $Me_4Pt(bpym)PtMe_4$

Pt1–C8	2.027(9)	Pt1–C7	2.051(10)
Pt1–C5	2.139(11)	Pt1–C6	2.125(9)
Pt1–N2a	2.147(8)	Pt1–N1	2.150(8)
C1–C1a	1.50(2)	Pt1–Pt1a	5.751(1)
C8–Pt1–C7	87.1(5)	C8–Pt1–C5	90.1(5)
C7–Pt1–C5	90.0(5)	C8–Pt1–C6	90.9(4)
C7–Pt1–C6	88.6(5)	C5–Pt1–C6	178.2(4)
C7–Pt1–N2a	97.6(4)	C6–Pt1–N2a	90.4(4)
N2a–Pt1–N1	77.2(3)		

Symmetry transformations used to generate equivalent atoms: −x, −y+1, −z.

The two most interesting features are the hardly shortened inter-ring bond length C1–C1a of 1.50 Å and the significantly longer metal–carbon axial bonds in comparison to the bonds to the equatorial methyl groups. The former effect reflects only a small degree of electron back donation from the electron-rich Pt–C_{ax} σ bond combinations into the π* system of the bpym acceptor which would increase the inter-ring bond order in the direction of a quinonoid formulation [10a]. The sizeable lengthening (and thus weakening) of the axial Pt–C bonds was observed previously [4e] for a mononuclear compound (α-diimine)$PtMe_4$; quantum mechanical calculations were thus employed here to reproduce and investigate this particular phenomenon.

The selected optimized DFT/HF bond lengths of $Me_4Pt(\mu\text{-bpym})PtMe_4$, $Me_2Pt(\mu\text{-bpym})PtMe_2$ and of the model system $H_4Pt(bpym)PtH_4$ (Table 4) are quite close to averaged values obtained from the experimental crystal structure.

The destabilization of Pt–Me_{ax} bonding is reflected by the calculated longer Pt–H_{ax} and Pt–Me_{ax} distances in comparison with equatorial bonds. Ab initio SCF procedures yield too long Pt–N bond distances (e.g. 2.277 Å for

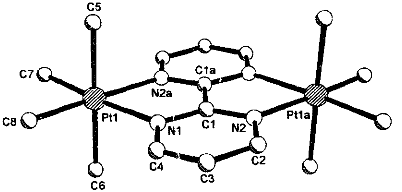

Fig. 1. Molecular structure representation of $Me_4Pt(bpym)PtMe_4$ from X-ray crystal structure analysis.

Table 4
Comparison of selected experimental bond lengths [a] in $Me_4Pt(\mu\text{-bpym})PtMe_4$] (A) and of DFT/HF-calculated values for $Me_4Pt(\mu\text{-bpym})PtMe_4$ (B), $H_4Pt(\mu\text{-bpym})PtH_4$ (C) and $Me_2Pt(\mu\text{-bpym})PtMe_2$ (D)

Bond	Exp. (A)	Calc. (B)	Calc. (C)	Calc. (D)
Pt–N [b]	2.149	2.192	2.196	2.172
N_1–C_1 [b]	1.336	1.355	1.346	1.346
N_2–C_2 [b]	1.359	1.344	1.343	1.343
C_2–C_3 [b]	1.367	1.393	1.397	1.397
C_1–C_{1A}	1.500	1.493	1.467	1.471
Pt–Me_{eq} [b]	2.039	2.062	1.551 [c]	2.046
Pt–Me_{ax} [b]	2.139	2.162	1.661 [c]	

[a] Bond lengths in Å.

[b] Average values for $Me_4Pt(\mu\text{-bpym})PtMe_4$.

[c] Calculated Pt–H bond lengths.

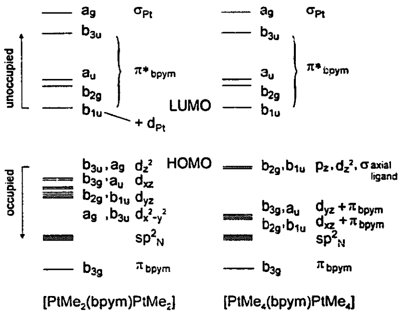

Fig. 2. DFT/HF-calculated one-electron MO energy diagrams of dinuclear Pt(II) and Pt(IV) compounds.

$H_4Pt(bpym)PtH_4$), while other bond parameters are reasonably well reproduced. DFT methods include electron correlation, and the better performance of the DFT method over non-correlated Hartree–Fock procedures points to the importance of electron correlation in these systems with their rather weak metal–diimine interaction. Due to the better performance of the DFT method all following results pertain to this method.

The calculated one-electron schemes for both kinds of Pt complexes as calculated by the DFT/HF method are shown in Fig. 2. The two almost degenerate highest-lying occupied MOs of $PtMe_4(\mu\text{-bpym})PtMe_4$ are mainly formed by the combinations of σ orbitals from the axial CH_3 ligands with the p_z and d_{z^2} orbitals of Pt (Fig. 3). The contribution of the bpym π system to these orbitals is less than 1%. The HOMO, b_{2g}, corresponds to the antisymmetrical combination and the second highest occupied MO, b_{1u}, to the symmetrical combination of p_z orbitals of Pt. The next sets of high-lying occupied orbitals can also be characterized as metal localized, completing the filled 't_{2g}' sets of d^6 centers (Pt^{IV}). The LUMO, b_{1u}, has essentially the same character as the first unoccupied π* orbital of free bpym, only very slightly perturbed by small contributions from p_z and d_{xz} orbitals of Pt.

The highest occupied MOs of $Me_2Pt(\mu\text{-bpym})PtMe_2$ are composed by a set of mainly metal-localized orbitals. The orbital of highest energy, b_{3u}, is mostly composed of d_{z^2} Pt orbitals, as depicted in Fig. 3(b). There are three close-lying pairs of other occupied metal-based orbitals in agreement with a square-planar d^8/d^8 metal configuration. The LUMO of $Me_2Pt(bpym)PtMe_2$ has a similar character as the corresponding orbital of $Me_4Pt(\mu\text{-bpym})PtMe_4$, yet in comparison there is a significantly larger contribution of Pt to this orbital (about 7%). Comparable numbers were extracted from analyses of EPR spectra of related systems [4i–k].

Summarizing, the reduction of both kinds of complexes should lead to acceptance of the single electron into the mainly μ-bpym-ligand localized π* orbital, b_{1u}, albeit with higher metal participation in the case of Pt(II) species. Due to the closely lying sets of HOMOs with energy separations of 0.05 eV or less, the oxidation of the complexes should result in two-electron processes, either from purely metal-based orbitals (d_{z^2}, Pt^{II}) or from metal-to-carbon σ bond combinations (→dissociation). In either case, the calculations suggest only very weak interaction of the metal fragments across the π-conjugated bpym ligand bridge.

3.3. Electrochemistry

In agreement with the identification of the LUMO as an acceptor orbital π* (b_{1u}) located on the bridging ligand, there are two reversible or at least quasi-reversible reduction processes observed for each of the four soluble complexes of Table 5.

Double metal coordination facilitates the reduction of bpym by about 1 V, in agreement with previous such observations [6,26]. However, there are significant similarities and differences. As was noted before [4e], analogous dimethylplatinum(II) and tetramethylplatinum(IV) derivatives exhibit almost identical first reduction potentials. Simply put, the addition of two carbanionic CH_3 co-substituents to the $PtMe_2$ fragment exactly offsets the effect of the increased oxidation state on the first reduction process of the bound α-diimine ligand [4e]. The second reduction potential, on the other hand, is significantly more negative for the

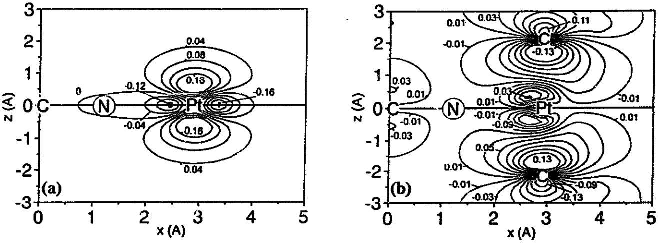

Fig. 3. DFT/HF-calculated contour maps of the HOMO in $Me_2Pt(bpym)PtMe_2$ (a, left) and in $Me_4Pt(bpym)PtMe_4$ (b, right; side views of one half of the molecules).

Table 5
Electrochemical data [a]

Compound	E_{pa}^{oxII} [b]	$E_{1/2}^{oxI}$ (ΔE_p) [c]	$E_{1/2}^{redI}$ (ΔE_p) [c]	$E_{1/2}^{redII}$ (ΔE_p) [c]
bpym			−2.31 (78)	−2.77 (irr.) [d]
(bpym)[$PtMe_4$]$_2$		0.43 (irr.) [b]	−1.34 (81)	−2.30 (84)
(bpym)[$PtMe_2$]$_2$		0.14 (irr.) [b]	−1.32 (87)	−2.04 (93)
(bpym)[$PtMes_2$]$_2$	1.17	0.57 (66) [e]	−1.18 (84)	−1.92 (105)
Mes_2Pt(bpym)$PtMe_4$	0.58 (72) [e,f]	0.46 (irr.) [b]	−1.26 (84)	−2.20 (95)

[a] From cyclic voltammetry in 0.1 M Bu_4NPF_6/THF solutions at 100 mV/s scan rate. Potentials in V vs. ferrocene/ferrocenium couple. No cyclic voltammogram could be obtained for Me_2Pt(bpym)$PtMes_2$ due to very poor solubility.

[b] Anodic peak potentials E_{pa} for irreversible oxidation.

[c] Half-wave potentials $E_{1/2}$, peak potential differences $\Delta E_p = E_{pa} - E_{pc}$ in mV (in parentheses).

[d] Cathodic peak potential E_{pc} for irreversible reduction.

[e] Two-electron process.

[f] Wave probably due to dissociation product.

bis(tetramethylplatinum(IV)) system, that very negative potential value reflecting the number of eight carbanionic groups present at the two metal centers.

The reduction of the dimesitylplatinum compounds is additionally facilitated by the partial acceptor effect of aryl substituents versus alkyl groups; however, the most interesting question here concerns the oxidation processes. Whereas the oxidation of Me_2Pt and Me_4Pt compounds is facile but irreversible due to multi-step oxidative addition (Pt^{II}) or dissociation processes (Pt^{IV}), the two mesityl substituents in Mes_2Pt complexes protect the axial positions of the square-planar metal center sufficiently to prevent attack from the solvent or from other molecules [4c,f]. Electrochemically reversible one-electron oxidation of compounds (α-diimine)$PtMes_2$ was thus shown to lead to persistent mononuclear Pt(III) species [4c,f] and the question posed here is whether *two* such processes can be observed for a symmetrically dinuclear ligand-bridged complex. Fig. 4 shows the cyclovoltammetric response, clearly demonstrating the occurrence of two simultaneous, reversible one-electron oxidations to yield [Mes_2Pt^{III}(bpym)$Pt^{III}Mes_2$]$^{2+}$. Due to the acceptor character of the aryl groups the potential lies somewhat positive in comparison to the anodic peak potentials of the alkyl complexes; a further but this time irreversible oxidation reaction takes place at still higher potentials (above 1 V versus $Fc^{+/0}$).

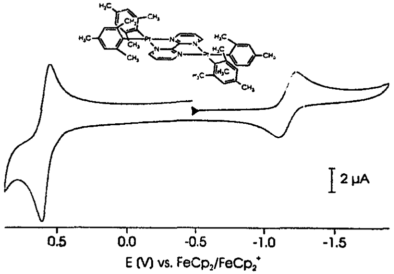

Fig. 4. Cyclic voltammogram of Mes_2Pt(bpym)$PtMes_2$ in THF/0.1 M Bu_4NPF_6 at 100 mV/s scan rate.

Differential pulse voltammetry (DPV) gave similar results as the cyclic voltammetric experiment. Obviously, there is no detectable communication between the HOMOs of the metal centers through the π system of the conjugated bridging ligand or, in other words, there is no stability of the Pt(III)/Pt(II) mixed-valent intermediate state. This observation for a d^7/d^8 system stands in contrast to results from d^5/d^6 mixed-valent species [6,27]. The reasons lie in the different character of the HOMOs: whereas complexes such as [L_4Ru(μ-bpym)RuL_4]$^{4+}$ have a d_π orbital as HOMO [27], the HOMO of R_2Pt(μ-bpym)PtR_2 is a σ-type orbital (d_{z^2}, Fig. 3(a)) which, in the present coordination arrangement, does not lend itself to metal–metal interaction as supported by the calculations (Fig. 2). In turn, these results support the notion of π acceptor mediated communication between the d^5/d^6 metal centers in corresponding compounds (electron transfer mechanism [6d,28]).

The electrochemical behavior of the mixed complex Mes_2Pt(μ-bpym)$PtMe_4$ confirms the ligand-based nature of the reduction (→averaged potentials) and the metal localization of the two different oxidation processes (→separate waves); similar observations had been reported on a number of heterodinuclear complexes L_nM(μ-bpym)$M'L'_n$ [26].

3.4. UV–Vis spectroscopy, solvatochromism and spectroelectrochemistry

The soluble bpym-bridged diplatinum complexes exhibit long-wavelength absorption maxima λ_1 around 600 nm (Table 6) which are attributed to either MLCT transitions $d_\pi \rightarrow \pi^*$(bpym) for the Pt^{II} species or to LLCT transitions σ(Pt–C) → π*(bpym) for the tetramethylplatinum(IV) species. According to the calculations presented here (Fig. 2) both kinds of transitions $b_{1u} \rightarrow b_{1u}$ are allowed. As has been outlined before [4e,f], the Pt(II) systems reveal partially structured CT bands due to a low number of degrees of freedom and thus better resolved vibrational structuring (Table 6).

Table 6
Long-wavelength absorption data [a]

Complex	λ_3 (ϵ)	λ_2 (ϵ)	λ_1 (ϵ)
(bpym)[$PtMe_4$]$_2$	372 sh	402 (2600) [b]	623 (1400)
(bpym)[$PtMes_2$]$_2$	362, 375 (10000)	432 (6300)	627 (3000) [c]
Mes_2Pt(bpym)$PtMe_4$	370 sh, 398 sh	428 sh, 511 sh	600 (2000)

[a] Wavelengths λ of maxima in nm, extinction coefficients ε in M^{-1} cm^{-1}; measurements in CH_2Cl_2. No spectra could be obtained for (bpym)[$PtMe_2$]$_2$ and Mes_2Pt(bpym)$PtMe_2$ due to insolubility.

[b] Shoulders at 430 and 458 nm.

[c] Further maxima at 573, 535 and 495 nm due to vibrational structuring.

Table 7
Franck–Condon contributions χ from intra- and intermolecular reorganization

Compound	$\Delta E = E^{ox}_{1/2} - E^{red}_{1/2}$ (V)	E_{op} (eV) [a]	χ [b]	Solvent
(bpym)$PtMes_2$ [c]	2.21	2.45	0.24	THF
(bpym)$PtMes_2$ [c]	2.11	2.57	0.46	MeCN
(bpym)[$PtMes_2$]$_2$	1.75	2.02	0.27	DCE
(bpym)[$PtMes_2$]$_2$	1.69	2.14	0.45	MeCN

[a] For long-wavelength absorption maxima λ_1, $E_{op} = c/\lambda_1$, 1 eV = 8065.5 cm^{-1}.

[b] $\chi = E_{op} - \Delta E$.

[c] From Ref. [4f].

Two further sets of intense bands λ_2 and λ_3 probably occur to higher unoccupied π* orbitals of the bpym ligand (Fig. 2); detailed assignments must await more elaborate techniques such as resonance Raman spectroscopy [29].

The mononuclear [4f] and dinuclear complexes (bpym)-[$PtMes_2$]$_{1,2}$ were studied in different solvents to quantify the obvious solvatochromic behavior of these compounds [3m,4b,c,f]. The long-wavelength absorption maxima λ_1 of the dinuclear species showed negative [30] solvatochromism with values of 650 nm (15 385 cm^{-1}, toluene), 627 nm (15 950 cm^{-1}, CH_2Cl_2), 613 nm (16 315 cm^{-1}, 1,2-dichloroethane), 585 nm (17 095 cm^{-1}, acetone), 578 nm (17 300 cm^{-1}, CH_3CN) and 567 nm (17 635 cm^{-1}, DMSO). Analysis of the relevant numbers in terms of a linear regression $\nu = A + B \times E^{*}_{MLCT}$, using the tested E^{*}_{MLCT} parameters [4b,c,f,30a,b], gave values $A = 14\,560$ cm^{-1} and $B = 2980$ cm^{-1} ($r = 0.997$). The sensitivity parameter B is close to that deduced for the mononuclear complex ($B = 3120$ cm^{-1}, $A = 17\,700$ cm^{-1} [4f]), confirming the concept put forward by Dodsworth and Lever [30c] on the significance of the *individual* metal–ligand dipolar arrangements even in symmetrical dinuclear complexes bridged by a π-conjugated ligand. The good correlation with E^{*}_{MLCT} rules out any specific π-type solvent–solute interaction [31], the mesityl groups shielding the square-planar Pt(II) centers.

Table 8
Spectroelectrochemical data: UV–Vis–NIR absorption maxima [a]

Complex ion	Absorption maxima
{(bpym)[$PtMe_4$]$_2$}$^{\cdot -}$ [b]	503, 954, 1124
{(bpym)[$PtMes_2$]$_2$}$^{\cdot -}$ [c]	488, 610 sh, 899
{Mes_2Pt(bpym)$PtMe_4$}$^{\cdot -}$ [b]	492, 525, 959, 1128
{(bpym)[$PtMe_4$]$_2$}$^{2-}$ [b]	380, 450 sh, 475 sh, 505 sh
{Mes_2Pt(bpym)$PtMe_4$}$^{2-}$ [b]	381, 415 sh, 453 sh, 493 sh
{(bpym)[$PtMes_2$]$_2$}$^{2+}$ [c]	775 [d], 1165 [d], 1420 [d]

[a] Wavelengths λ in nm.

[b] Generated by in situ electrolysis in THF/0.1 M Bu_4NPF_6 at ambient temperatures.

[c] Measured in 1,2-dichloroethane/0.1 M Bu_4NPF_6.

[d] Ligand-field transitions of low-spin d^7 system, extinction coefficients $\epsilon < 1000$ M^{-1} cm^{-1}.

The mononuclear [4f] and dinuclear complexes (bpym)-[$PtMes_2$]$_{1,2}$ were also studied in two different solvents with respect to correlating electrochemical and optical properties. The availability of both half-wave potentials for reversible oxidation and reduction allowed us to calculate approximate numbers χ for the contributions from intra- and intermolecular reorganization [4f,32] by subtracting values $\Delta E = E^{ox}_{1/2} - E^{red}_{1/2}$ (in V) for the geometrically relaxed states from values E_{op} (in eV) for the long-wavelength absorption maximum (ground-state geometry according to the Franck–Condon principle [32]). The values summarized in Table 7 illustrate very comparable behavior of mono- and dinuclear complexes (see above) and a characteristic effect of the solvent (intermolecular reorganization). The calculated χ is higher in the more polar acetonitrile, whereas the value of about 0.25 (e)V in DCE indicates a rather small degree of geometrical reorganization [32b] — in agreement with the apparently rigid structure [4c,f].

The persistence of one- and two-electron reduced species and, in the case of Mes_2Pt(bpym)$PtMes_2$, of the two-electron oxidized form allowed us to study these states by UV–Vis–NIR spectroelectrochemistry [4f,17]. Isosbestic points during corresponding experiments and the full reconstitution of absorption bands after re-oxidation or re-reduction confirmed the validity of these measurements. The absorption maxima listed in Table 8 are in agreement with data reported previously for bis(organoplatinum) or other dinuclear transition metal complexes of bpym$^{\bullet-}$ and bpym^{2-} [4a,d,33]. The radical complexes are distinguished by broad, sometimes vibrationally structured bands in the NIR region originating from symmetry-forbidden intra-ligand transitions [4a,33]. The dianionic species, on the other hand, exhibit fairly high energy intra-ligand transitions. In all cases, the long-wavelength charge transfer transitions are diminished or shifted to higher energies.

The MLCT feature is also shifted hypsochromically on oxidation of Mes$_2$Pt(bpym)PtMes$_2$; however, there are now three weak bands appearing in the long-wavelength region which are attributed to ligand-field (d→d) transitions of low-spin d^7 centers [4f,34]. The absorption maxima (Table 8) are not very different from those observed for mononuclear species [(α-diimine)PtMes$_2$]$^+$ [4f], confirming the negligible degree of metal–metal interaction.

3.5. EPR spectroscopy

Reversible two-electron oxidation of Mes$_2$Pt(bpym)-PtMes$_2$ produces a dication which did not exhibit an EPR signal, either at room temperature or in frozen 1,2-dichloroethane solution at 3.5 K. Similarly, even mononuclear complexes [(α-diimine)PtMes$_2$]$^+$ remained EPR silent [4f] which was attributed to very rapid relaxation caused by close-lying states and a high spin–orbit coupling constant of the metal [35]. We can thus only speculate whether the absence of EPR signals has similar causes or whether there is additional spin–spin interaction between the two 5d^7 centers which are separated by about 5.7 Å.

Reversible reduction of the soluble diplatinum complexes of 2,2′-bipyrimidine produces broad EPR signals at room temperature. All isotropic g factors lie below 2, indicating contributions from close-lying excited states with non-zero orbital angular momentum to the doublet ground state [10a]. The question as to whether these species contain Pt$^{\mathrm{I}}$ [4d–j] or Pt$^{\mathrm{III}}$ [4f,36] configurations is best answered on the basis of EPR studies in frozen solution (Fig. 5, Table 9).

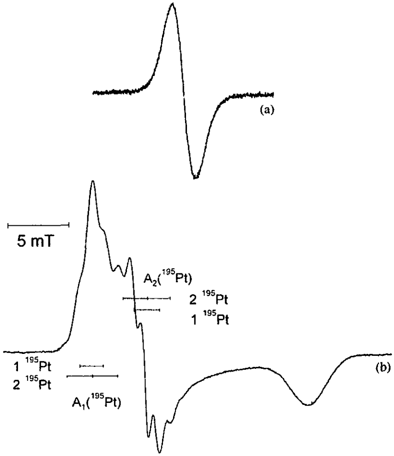

Fig. 5. EPR spectra of [Mes$_2$Pt(bpym)PtMe$_4$]$^{\bullet-}$, electrogenerated in THF/0.1 M Bu$_4$NPF$_6$ in fluid solution at 300 K (a) and in the glassy frozen state at 110 K (b).

Fig. 5 illustrates that the systems exhibit rhombic g anisotropy in the frozen state with one particular low g component (g_3) [4g,j,k]; the other two components exhibit metal hyperfine coupling from the ^{195}Pt isotope. Due to the presence of two such metal nuclei there are three relevant isotope combinations, ^{195}Pt/^{195}Pt, ^{195}Pt/^{19x}Pt and ^{19x}Pt/^{19x}Pt (x=0, 2, 4, 6, 8, 66.2%, I=0; ^{195}Pt, 33.8%, I=1/2). While the latter combinations produce only a single EPR resonance line, the combinations with one or two ^{195}Pt nuclei cause a splitting into two or three lines, respectively (Fig. 5), resulting formally in a quintet. Interestingly, both the dimesitylplatinum(II) and tetramethylplatinum(IV) centers exhibit anisotropic hyperfine components a_1 and a_2 of a comparable, relatively [4] small magnitude (Table 9), thus supporting the formulation of even-electron metal fragments bound to

Table 9
EPR data [a] of anionic dinuclear organoplatinum complexes

Compound [b]	g_{iso} [c]	g_1	g_2	g_3	Δg [d]	Solvent
{(bpym)[PtMes$_2$]$_2$}$^{\bullet-}$	1.9915	2.0435	2.0091 [e]	1.916	0.1275	DCE
{(bpym)[PtMe$_4$]$_2$}$^{\bullet-}$	1.9887	2.010	2.0053	1.950	0.060	DCE
{Mes$_2$Pt(bpym)PtMe$_4$}$^{\bullet-}$	1.9891	2.030 [f]	2.0048 [g]	1.930	0.100	THF

[a] Coupling constants a in mT (1 T = 10^4 G).

[b] Generated by in situ electrolysis at ambient temperatures in 0.1 M Bu$_4$NPF$_6$–solvent systems. No EPR spectra could be obtained from electrolysis of the compounds (bpym)[PtMe$_2$]$_2$ and Mes$_2$Pt(bpym)PtMe$_2$ due to poor solubility.

[c] ^{195}Pt, I = 1/2, 33.8% nat. abundance. g_{iso} measured at room temperature, anisotropic g factors and coupling constants at 110 K.

[d] $\Delta g = g_1 - g_3$.

[e] a_2(Pt) = 1.6 mT.

[f] a_1(Pt) = 1.7 mT (average).

[g] a_2(Pt) = 1.85 mT (average).

bpym$^{\bullet -}$. In relation to the anisotropic hyperfine coupling constant A_{iso} = 1227.84 mT [35], the observed values of less than 2 mT confirm the low participation of the metal centers at the singly occupied MO [4e–k,37].

A more detailed picture results when the total g anisotropies Δg of the Pt(II) and Pt(IV) species are compared. The large spin–orbit coupling constant of Pt [35] causes a fairly large and very diagnostic [4g] splitting of g components which, however, is distinctly larger for the Pt(II) system [4e]. This observation points to a higher degree of metal participation at the singly occupied b_{1u} MO, as was suggested by the DFT calculations (Section 3.1). Nevertheless, neither Pt(I) = d^9 nor Pt(III) = d^7 species are obtained on reduction of these organoplatinum complexes of bpym; true organoplatinum(III) species, as generated by metal-centered oxidation (see above) or otherwise, should exhibit different EPR characteristics [8a,36].

4. Conclusions

We have demonstrated in this work how different organoplatinum(II) and -(IV) fragments can bind to conjugated bridging 2,2′-bipyrimidine in various oxidation states. While the anionic forms contain bpym-centered additional electrons, the oxidation occurs either at the metal (Pt^{II}) or from the platinum–carbon bonds (Pt^{IV}). Due to the particular orbital situation of the Pt(II) systems there are few extra effects in comparison to corresponding mononuclear systems; however, it remains to be studied whether bridging ligands with stronger metal–metal coupling capability [28] than bpym can cause a splitting of the one-electron oxidation waves of two coordinated Mes_2Pt fragments. Another open question is that of possible emissive behavior [3] in the NIR region which requires sensitive detection techniques.

Acknowledgements

This work was supported by a grant from Volkswagenstiftung and by the Fonds der Chemischen Industrie.

References

[1] (a) N. Farrell, in B.R. James and R. Ugo (eds.), *Transition Metal Complexes as Drugs and Chemotherapeutic Agents*, Reidel–Kluwer, Dordrecht, 1989, p. 46; (b) M.J. Bloemink and J. Reedijk, in H. Sigel and A. Sigel (eds.), *Metal Ions in Biological Systems*, Vol. 32, Marcel Dekker, New York, 1996, p. 641; (c) W.I. Sundquist and S.J. Lippard, *Coord. Chem. Rev., 100* (1990) 293.

[2] S.S. Stahl, J.A. Labinger and J.E. Bercaw, *J. Am. Chem. Soc., 118* (1996) 5961.

[3] (a) V.M. Miskowski and V.H. Houlding, *Inorg. Chem., 28* (1989) 1529; (b) C.-M. Che, L.-Y. He, C.-K. Poon and C.W. Mak, *Inorg. Chem., 28* (1989) 3081; (c) J. Biedermann, G. Gliemann, U. Klement, K.-J. Range and M. Zabel, *Inorg. Chem., 29* (1990) 1884; (d) J. Biedermann, G. Gliemann, U. Klement, K.-J. Range and M. Zabel, *Inorg. Chim. Acta, 169* (1990) 63; (e) H. Kunkely and A. Vogler, *J. Am. Chem. Soc., 112* (1990) 5625; (f) V.M. Miskowski and V.H. Houlding, *Inorg. Chem., 30* (1991) 4446; (g) L. Chassot and A. von Zelewsky, *Helv. Chim. Acta, 69* (1986) 1855; (h) V.M. Miskowski, V.H. Houlding, C.M. Che and Y. Wang, *Inorg. Chem., 32* (1993) 2518; (i) V.H. Houlding and V.M. Miskowski, *Coord. Chem. Rev., 111* (1991) 145; (j) C. Cornioley-Deuschel and A. von Zelewsky, *Inorg. Chem., 26* (1987) 3354; (k) A. von Zelewsky, P. Belser, P. Hayoz, R. Dux, X. Husa, A. Suckling and H. Stoeckli-Evans, *Coord. Chem. Rev., 132* (1994) 75; (l) C.-W. Chan, L.-K. Cheng and C.-M. Che, *Coord. Chem. Rev., 132* (1994) 87; (m) S.D. Cummings and R. Eisenberg, *J. Am. Chem. Soc., 118* (1996) 1949; (n) C.S. Peyratout, T.K. Aldridge, D.K. Crites and D.R. McMillin, *Inorg. Chem., 34* (1995) 4484; (o) W.B. Connick, L.M. Henling, R.E. Marsh and H.B. Gray, *Inorg. Chem., 35* (1996) 6261.

[4] (a) P.S. Braterman, J.-I. Song, C. Vogler and W. Kaim, *Inorg. Chem., 31* (1992) 222; (b) C. Vogler, B. Schwederski, A. Klein and W. Kaim, *J. Organomet. Chem., 436* (1992) 367; (c) A. Klein, H.-D. Hausen and W. Kaim, *J. Organomet. Chem., 440* (1992) 207; (d) P.S. Braterman, J.-I. Song, F.M. Wimmer, S. Wimmer, W. Kaim, A. Klein and R.D. Peacock, *Inorg. Chem., 31* (1992) 5084; (e) S. Hasenzahl, H.-D. Hausen and W. Kaim, *Chem. Eur. J., 1* (1995) 95; (f) W. Kaim and A. Klein, *Organometallics, 14* (1995) 1176; (g) A. Klein, W. Kaim, E. Waldhör and H.-D. Hausen, *J. Chem. Soc., Perkin Trans. 2*, (1995) 2121; (h) R.J. Klinger, R.J. Huffman and J.K. Kochi, *J. Am. Chem. Soc., 104* (1982) 2147; (i) S.A. MacGregor, E. McInnes, R.J. Sorbie and L.J. Yellowlees, in A.J.L. Pombeiro and J.A. McCleverty (eds.), *Molecular Electrochemistry of Inorganic, Bioinorganic and Organometallic Compounds*, Kluwer, Dordrecht, 1993, p. 503; (j) D. Collison, F.E. Mabbs, E.J.L. McInnes, K.J. Taylor, A.J. Welch and L.J. Yellowlees, *J. Chem. Soc., Dalton Trans.*, (1996) 329; (k) M.G. Hill, J.A. Bailey, V.M. Miskowski and H.B. Gray, *Inorg. Chem., 35* (1996) 4585; (l) E.J.L. McInnes, A.J. Welch and L.J. Yellowlees, *J. Chem. Soc., Chem. Commun.*, (1996) 2393.

[5] V. Balzani, A. Juris, M. Venturi, S. Campagna and S. Serroni, *Chem. Rev., 96* (1996) 759.

[6] (a) W. Kaim and S. Kohlmann, *Inorg. Chem., 26* (1987) 68; (b) S.D. Ernst and W. Kaim, *Inorg. Chem., 28* (1989) 1520; (c) W. Kaim and S. Kohlmann, *Inorg. Chem., 29* (1990) 2909; (d) W. Kaim and V. Kasack, *Inorg. Chem., 29* (1990) 4696.

[7] (a) P.J. Stang, D.H. Cao, S. Saito and A.M. Arif, *J. Am. Chem. Soc., 117* (1995) 6273; (b) J.K. Barton, D.J. Szalda, M.N. Rabinowitz, J.V. Waszczak and S.J. Lippard, *J. Am. Chem. Soc., 101* (1979) 1434; (c) W. Micklitz, G. Müller, B. Huber, J. Riede, F. Rashwan, J. Heinze and B. Lippert, *J. Am. Chem. Soc., 110* (1985) 70 684; (d) K. Matsumoto, K. Sakai, K. Nishio, Y. Tokisue, R. Ito, T. Nishide and Y. Shichi, *J. Am. Chem. Soc., 114* (1992) 8110; (e) R. Usón, J. Forniés, L.R. Falvello, M. Tomás, J.M. Casas, A. Martín and F.A. Cotton, *J. Am. Chem. Soc., 116* (1994) 7160; (f) J. Forniés, B. Menjón, R.M. Sanz-Carrillo, M. Tomás, N.G. Connelly, J.G. Crossley and A.G. Orpen, *J. Am. Chem. Soc., 117* (1995) 4295; (g) P.D. Prenzler, G.A. Heath, S.B. Lee and R.G. Raptis, *J. Chem. Soc., Chem. Commun.*, (1996) 2271.

[8] (a) R. Usón, J. Forniés, M. Tomás, J.M. Casas, F.A. Cotton, L.R. Falvello and X. Feng, *J. Am. Chem. Soc., 115* (1993) 4145; (b) F.A. Cotton, J.H. Matonic and C.A. Murillo, *Inorg. Chem., 35* (1996) 498.

[9] (a) N. Farrell, *Comments Inorg. Chem., 16* (1995) 373; (b) E. Schuhmann, J. Altman, K. Karaghiosoff and W. Beck, *Inorg. Chem., 34* (1995) 2316.

[10] (a) W. Kaim, *Inorg. Chem., 23* (1984) 3365; (b) M. Schwach, H.-D. Hausen and W. Kaim, *Chem. Eur. J., 2* (1996) 446; (c) G. De Munno, T. Poerio, G. Viau, M. Julve, F. Lloret, Y. Journaux and E. Rivière, *J. Chem. Soc., Chem. Commun.*, (1996) 2587.

[11] J.D. Scott and R.J. Puddephatt, *Organometallics, 5* (1986) 1538.

[12] (a) M. Bochmann, G. Wilkinson and G.B. Young, *J. Chem. Soc., Dalton Trans.*, (1980) 1879; (b) V.F. Sutcliffe and G.B. Young, *Polyhedron, 3* (1984) 87, and Refs. therein.

[13] C. Eaborn, K. Kundu and A. Pidcock, *J. Chem. Soc., Dalton Trans.*, (1981) 933.

[14] M. Lashanizadeghan, M. Rashidi, J.E. Hux, R.J. Puddephatt and S.S.M. Ling, *J. Organomet. Chem.*, *269* (1984) 317.

[15] J.D. Scott and R.J. Puddephatt, *Organometallics*, *2* (1983) 1643.

[16] F.A. Cotton, R. Francis and W.D. Horrocks, Jr., *J. Phys. Chem.*, *64* (1960) 1534.

[17] M. Krejčik, M. Danek and F. Hartl, *J. Electroanal. Chem.*, *317* (1991) 179.

[18] W. Kaim, S. Ernst and V. Kasack, *J. Am. Chem. Soc.*, *112* (1990) 173.

[19] M.J. Frisch, G.W. Trucks, H.B. Schlegel, P.M.W. Gill, B.G. Johnson, M.A. Robb, J.R. Cheeseman, T.A. Keith, J.A. Peterson, J.A. Montgomery, K. Raghavachari, M.A. Al-Laham, V.G. Zakrezewski, J.V. Oritz, J.B. Foresman, J. Cioslowski, B. Stefanov, A. Nanayakkara, M. Challacombe, C.Y. Peng, P.Y. Ayala, W. Chen, M.W. Wong, J.L. Andres, E.S. Replogle, R. Gomperts, R.L. Martin, D.J. Fox, J.S. Binkley, D.J. Defrees, J. Baker, J.P. Stewart, M. Head-Gordon, C. Gonzales and J.A. Pople, *Gaussian 94*, Revision B.3, Gaussian, Inc., Pittsburgh, PA, 1995.

[20] D. Andrae, U. Häußermann, M. Dolg, H. Stoll and H. Preuß, *Theor. Chim. Acta*, *77* (1990) 123.

[21] T.H. Dunning and P.J. Hay, *Modern Theoretical Chemistry*, Plenum, New York, 1977.

[22] A.D. Becke, *J. Chem. Phys.*, *98* (1993) 5648.

[23] (a) G.M. Sheldrick, *SHELXTL-Plus*, an integrated system for solving, refining and displaying crystal structures from diffraction data, Siemens Analytical X-Ray Instruments Inc., 1989; (b) G.M. Sheldrick, *SHELXL-93*, program for crystal structure determination, Universität Göttingen, 1993; (c) N. Walker and D. Stuart, *Acta Crystallogr., Sect. A*, *39* (1983) 158.

[24] S. Hasenzahl, W. Kaim and T. Stahl, *Inorg. Chim. Acta*, *225* (1994) 23.

[25] (a) A. Klein, S. Hasenzahl and W. Kaim, *J. Chem. Soc., Faraday Trans.*, in press; (b) W. Kaim, A. Klein, S. Hasenzahl, H. Stoll, S. Zalis and J. Fielder, *Organometallics*, submitted for publication.

[26] W. Matheis and W. Kaim, *Inorg. Chim. Acta*, *181* (1991) 15.

[27] (a) M. Hunzicker and A. Ludi, *J. Am. Chem. Soc.*, *99* (1977) 7370; (b) R.R. Ruminski and J.D. Petersen, *Inorg. Chem.*, *21* (1982) 3706; (c) F. Baumann, W. Kaim, N.E. Katz, M. Garcia Posse and J. Fiedler, *Inorg. Chem.*, submitted for publication.

[28] S. Ernst, V. Kasack and W. Kaim, *Inorg. Chem.*, *27* (1988) 1146.

[29] W. Kaim, S. Kohlmann, A.J. Lees, T.L. Snoeck, D.J. Stufkens and M.M. Zulu, *Inorg. Chim. Acta*, *210* (1993) 159.

[30] (a) C.M. Manuta and A.J. Lees, *Inorg. Chem.*, *22* (1983) 3825; (b) W. Kaim, S. Kohlmann, S. Ernst, B. Olbrich-Deussner, C. Bessenbacher and A. Schulz, *J. Organomet. Chem.*, *321* (1987) 215; (c) E.S. Dodsworth and A.B.P. Lever, *Coord. Chem. Rev.*, *97* (1990) 271; E.S. Dodsworth and A.B.P. Lever, *Inorg. Chem.*, *29* (1990) 499.

[31] W. Kaim, B. Olbrich-Deussner and T. Roth, *Organometallics*, *10* (1991) 410.

[32] (a) E.M. Kober, K.A. Goldsby, D.N.S. Narayana and T.J. Meyer, *J. Am. Chem. Soc.*, *105* (1983) 4303; (b) E.S. Dodsworth and A.B.P. Lever, *Chem. Phys. Lett.*, *119* (1985) 61; *124* (1986) 152.

[33] P.S. Braterman, J.-I. Song, S. Kohlmann, C. Vogler and W. Kaim, *J. Organomet. Chem.*, *411* (1991) 207.

[34] (a) For a discussion, see: A. Ceulemans, M. Dendooven and L.G. Vanquickenborne, *Inorg. Chem.*, *24* (1985) 1159; (b) L. Falvello and M. Gerloch, *Inorg. Chem.*, *19* (1980) 472.

[35] J.A. Weil, J.R. Bolton and J.E. Wertz, *Electron Paramagnetic Resonance*, Wiley, New York, 1994.

[36] (a) R. Uson, J. Fornies, M. Tomas, B. Menjon, R. Bau, K. Sünkel and E. Kuwabara, *Organometallics*, *5* (1986) 1576; (b) R. Uson, J. Fornies, M. Tomas, I. Ara and B. Menjon, *J. Organomet. Chem.*, *226* (1987) 129; (c) A.J. Blake, R.O. Gould, A.J. Holder, T.I. Hyde, A.J. Lavery, M.O. Odulate and M. Schröder, *J. Chem. Soc., Chem. Commun.*, (1987) 118; (d) A.J. Blake, A.J. Holder, T.I. Hyde and M. Schröder, *J. Chem. Soc., Chem. Commun.*, (1987) 987; (e) K.K. Pandey, *Coord. Chem. Rev.*, *121* (1992) 1; (f) M. Geoffroy, G. Bernardinelli, P. Castan, H. Chermette, D. Deguenon, S. Nour, J. Weber and M. Wermeille, *Inorg. Chem.*, *31* (1992) 5056; (g) M. Wermeille, M. Geoffroy, P. Arrizabalaga and G. Bernardinelli, *Inorg. Chim. Acta*, *211* (1993) 81; (h) W.L. Waltz, J. Lilie, R.T. Walters and R.J. Woods, *Inorg. Chem.*, *19* (1980) 3284; (i) H.A. Boucher, G.A. Lawrance, P.A. Lay, A.M. Sargeson, A.M. Bond, D.F. Sangster and J.C. Sullivan, *J. Am. Chem. Soc.*, *105* (1983) 4652.

[37] W. Kaim, *Coord. Chem. Rev.*, *76* (1987) 187.